Journal of Power Sources 195 (2010) 2570–2578

Contents lists available at ScienceDirect

Journal of Power Sources

journal homepage: www.elsevier.com/locate/jpowsour

Syntheses, characterization, and catalytic oxygen electroreduction activities of carbon-supported PtW nanoparticle catalysts

Liufeng Xiong[a], Karren L. More[b], Ting He[a,*]

[a] Honda Research Institute USA, Inc., 1381 Kinnear Rd., Columbus, OH 43212, USA
[b] Materials Science and Technology Division, Oak Ridge National Laboratory, Oak Ridge, TN 37831, USA

ARTICLE INFO

Article history:
Received 14 October 2009
Received in revised form 2 November 2009
Accepted 3 November 2009
Available online 10 November 2009

Keywords:
PtW
Fuel cell
ORR
Electrocatalyst
Synthesis

ABSTRACT

Carbon-supported PtW (PtW/C) alloy nanoparticle catalysts with well-controlled particle size, dispersion, and composition uniformity, have been synthesized by wet chemical methods of decomposition of carbonyl cluster complexes, hydrolysis of metal salts, and chemical reactions within a reverse microemulsion. The synthesized PtW/C catalysts were characterized by X-ray diffraction, high-resolution transmission electron microscopy, and energy-dispersive spectroscopy. The catalytic oxygen electroreduction activities were measured by the hydrodynamic rotating disk electrode technique in an acidic electrolyte. The influence of the synthesis method on PtW particle size, size distribution, composition uniformity, and catalytic oxygen electroreduction activity, have been investigated. Among the synthesis methods studied, PtW/C catalysts prepared by the decomposition of carbonyl cluster complexes displayed the best platinum mass activity for oxygen reduction reaction under the current small scale production; a 3.4-fold catalytic enhancement was achieved in comparison to a benchmark Pt/C standard.

1. Introduction

The direct conversion of chemical energy to electricity via fuel cells has attracted significant attention for many decades [1–6]. Of the electrochemical reactions involved in the energy conversion in low temperature fuel cells, the oxygen reduction reaction (ORR) is the rate-determining process. Even for current state-of-the-art platinum (Pt) catalysts, the exchange current density for the ORR is several orders of magnitude smaller than that for the hydrogen oxidation reaction (HOR), resulting in a dramatic loss in energy conversion efficiency. Consequently, oxygen electroreduction technology is regarded as the key issue for developing viable low temperature fuel cells for stationary, portable, and transportation applications [7].

Recently, significant progress has been made in the development of Pt and Pt alloy electrocatalysts [8–15]. By alloying Pt with 3d transition metals, a ten-fold catalytic activity enhancement towards molecular oxygen electroreduction has been achieved for Pt alloy model catalysts (thin films) as compared to a pure Pt thin film standard [8,15]. However, due to challenges in tailoring Pt alloy particles at the nanoscale – particularly in controlling alloy particle size and micro-compositional uniformity – such high catalytic activities have never been demonstrated in actual fuel cells.

Platinum tungsten (PtW) alloys were originally proposed as oxidation electrocatalysts (anode catalysts) for polymer electrolyte membrane fuel cells (PEMFCs) operated with methanol, ethanol, or reformate gases [16–18]. A high throughput combinatorial study performed recently in our laboratory demonstrated that PtW alloy films also present superior catalytic activities towards molecular oxygen electroreduction, with a 4-fold catalytic activity enhancement over pure Pt for a PtW alloy having a Pt:W molar ratio of 1:2 [19,20]. In comparison with other Pt alloy electrocatalyst candidates, PtW offers several advantages: (i) the amount of Pt can be reduced dramatically due to low Pt content (~35 wt%) in the PtW (1:2) alloy, whereas other PtM alloys (with a Pt:M of 3:1, where M = Co, Ni, Ti, etc.) have Pt contents greater than 90 wt%; (ii) W has high tolerances towards anode catalyst poisons [21], i.e., W will not damage a fuel cell even if it diffuses to the anode due to dissolution; and (iii) a recent study showed that W can also function as catalyst for hydrogen peroxide decomposition, thus potentially inhibiting membrane damage due to hydrogen peroxide formation [22].

The most common methods to synthesize PtW alloy nanoparticles are impregnation and chemical co-reduction of chloroplatinic acid and ammonium tungstate [16,17]. However, both synthesis methods are not effective for preparing PtW alloy nanoparticles with well-controlled particle sizes and compositions. For instance, the impregnation method is not conducive for controlling particle size and compositional homogeneity [16] and the chemical reduction method does not completely reduce tungsten to its metallic state, even when utilizing very strong reducing agents [18].

* Corresponding author. Tel.: +1 614 327 4767; fax: +1 614 340 6082.
E-mail address: the@honda-ri.com (T. He).

0378-7753/$ – see front matter © 2009 Elsevier B.V. All rights reserved.
doi:10.1016/j.jpowsour.2009.11.013

In an earlier report, we demonstrated that carbon-supported PtW alloy nanoparticles could be synthesized with carbonyl precursors and the resulting catalysts exhibited superior catalytic oxygen reduction activities [23]. In this paper, details of synthesizing carbon-supported PtW alloy nanoparticle catalysts by various wet chemical methods will be reported and the influence of synthesis methods on particle size, size distribution, nanoparticle dispersion, composition uniformity, and catalytic oxygen reduction activity will be discussed.

2. Experimental

2.1. Synthesis methods

Three wet chemical methods – decomposition of carbonyl cluster complexes (CBN), hydrolysis of Pt and W salts in aqueous solution (HYD), and reduction of Pt and hydrolysis of W precursors within nano-reactors of a reverse microemulsion (RME) – have been developed to synthesize carbon-supported PtW alloy nanoparticle catalysts, the details of which are given in the following sections.

2.1.1. Carbonyl method (CBN)

The synthesis of carbon-supported PtW alloy nanoparticle catalysts by thermal decomposition of platinum and tungsten carbonyl cluster complexes under a controlled atmosphere was previously reported by this group [23], and similar method was reported to fabricate other Pt binary alloys [24–27]. The basic concept is a bottom up approach that can be intuitively described by:

$$[Pt_3(CO)_6]_n + W(CO)_6 \rightarrow [Pt_xW_y(CO)_z] \rightarrow Pt_xW_y$$

Briefly, the synthesis procedure involves following steps:

I. Preparation of platinum carbonyl: Platinum carbonyl was prepared by chemical reaction of chloroplatinic acid (H_2PtCl_6, Aldrich) with carbon monoxide (CO) in tetrahydrofuran (THF). Chloroplatinic acid was dissolved in THF followed by 24 h of CO purging (50 ml min^{-1}) under constant mechanical stirring. The color of the Pt-THF solution slowly changed from orange to dark green to black indicating the end of the reaction.
II. Formation of bimetallic carbonyl cluster complexes: Commercially available tungsten carbonyl ($W(CO)_6$, Aldrich) was dissolved in THF and added to the prepared platinum carbonyl solution. The mixture was further purged with CO for an additional 2 h under constant mechanical stirring resulting in the formation of bimetallic carbonyl cluster complexes.
III. Dispersion on carbon-supports: An appropriate amount of carbon black (Ketjen Black International), dispersed in THF by ultrasonication, was added to the Pt/W-THF solution under constant CO purging and mechanical stirring until an uniform solution was achieved.
IV. Removal of solvent: THF was slowly evaporated by blowing a mixture of CO and N_2 under constant mechanical stirring.
V. Thermal decomposition of carbonyl cluster complexes and alloying bimetallic nanoparticles: After the solvent was evaporated, the powder was collected and heat-treated at temperatures ranging from 500 °C to 800 °C for 2 h under flowing mixture of H_2/N_2 (1:10, v/v). Carbonyl cluster complexes were decomposed at relatively low temperatures (<200 °C) and high temperatures were needed to create truly alloyed nanoparticles.

Carbon-supported PtW alloy nanoparticles of different compositions were synthesized by manipulating the relative concentrations of chloroplatinic acid and tungsten carbonyl. A representative procedure of, for example, preparing 175 mg carbon-supported PtW (52:48) nanoparticle catalyst with an alloy loading of 40 wt% includes: dissolving 0.315 ml chloroplatinic acid (0.61 mM ml^{-1}) in 100 ml THF followed by 24 h of CO purging under constant mechanical stirring; adding 62.4 mg $W(CO)_6$ to the Pt-THF solution followed with an additional 2 h CO purging; ultrasonically dispersing 105 mg carbon in 20 ml THF and mixing with the Pt/W-THF solution; evaporating the solvent by blowing a mixture of CO/N_2 under constant mechanical stirring; and heat treating the powders at 700 °C for 2 h under a flowing mixture of H_2/N_2 (1:10, v/v). The first two rows of Table 1 show the PtW/C catalysts prepared by this method.

Table 1
Characteristic parameters of various carbon-supported PtW alloy nanoparticle catalysts synthesized by the three wet chemical approaches. The activity of the benchmark Pt/C standard at 0.8 V is 934.2 mA cm^{-2} mg_{Pt}^{-1} with a half-wave potential of 800 mV. The particle sizes are estimated from XRD broadening and the metal loadings are referred to PtW alloy loadings.

Synthesis method	Pt:W	Alloying temp. (°C)	Particle size (nm)	Loading (wt%)	Relative activity (0.8 V)	$\Delta E_{1/2}$ (mV)
CBN	69:31	700	2.7	39.8	2.2	24.8
	60:40	700	3.2	33.8	2.2	9.8
	52:48	700	2.6	41.5	2.5	14.6
	46:54	700	3.0	41.0	2.3	19.8
	39:61	700	3.5	42.8	3.4	19.7
	28:72	700	4.7	31.0	2.6	−20.7
CBN	52:48	500	2.3	39.9	1.3	−14.1
		600	2.5	40.5	1.5	−6.0
		700	2.6	41.5	2.5	14.6
		800	13.8	42.0	1.4	−12.0
HYD	68:32	700	2.2	31.2	2.4	16.7
	54:46	700	3.0	38.0	2.5	14.5
	40:60	700	2.5	41.8	2.7	11.2
	28:72	700	3.2	42.6	3.0	2.2
RME (AOT)	51:49	25	3.3	–	–	–
		700	6.8	–	–	–
		900	8.1	41.4	1.0	−17.1
RME (Brij30)	53:47	700	3.9	38.2	1.7	−0.2
	38:62	700	–	36.2	2.3	−6.5
	32:68	700	3.9	43.9	2.9	2.4
	23:76	700	–	44.6	2.6	−18.6

2.1.2. Hydrolysis method (HYD)

Carbon-supported PtW alloy nanoparticle catalysts were also synthesized by hydrolysis of chloroplatinic acid (H_2PtCl_6, Aldrich) and sodium tungstate (Na_2WO_4, Aldrich) in de-ionized water. The key steps are to control pH, temperature, and hydrolysis time [28]. The synthesis procedure involves the following three steps:

I. Hydrolysis of chloroplatinic acid in a base medium: Appropriate amounts of chloroplatinic acid, sodium tungstate, and carbon black were dissolved/dispersed in de-ionized water under constant mechanical stirring. The pH of the solution was adjusted to 10 by drop-wise adding ammonium hydroxide. The mixture was then ultrasonically blended for 15 min prior to hydrolysis at 70 °C for 20 h. A colloidal platinum stabilized by hydroxyl ions was obtained.
II. Hydrolysis of sodium tungstate in an acid solvent: After hydrolysis of chloroplatinic acid in the base environment, the Pt/W solution was cooled to room temperature. The pH of the solution was then adjusted to 3 by the drop-wise addition of concentrated nitric acid. The solution was kept under constant mechanical stirring for hydrolysis for an additional 2 h resulting in co-precipitated platinum and tungsten on the carbon-supports. The precipitated product was further filtered, washed with de-ionized water, and dried in a furnace.
III. Formation of PtW alloys: The synthesized platinum and tungsten containing powder was heat-treated at 700 °C for 2 h under a flowing mixture of H_2/N_2 (1:10, v/v). During the heat treatment, platinum and tungsten were reduced to metallic states and PtW alloys were formed.

The third row of Table 1 displays the PtW/C catalysts synthesized by the hydrolysis method. In a typical procedure for the synthesis of 500 mg of carbon-supported 40 wt% PtW (28:72) nanoparticle catalyst, for instance, 0.6 ml chloroplatinic acid (0.61 mM ml^{-1}), 280 mg sodium tungstate, and 50 ml de-ionized water were added to a 250 ml flask under constant mechanical stirring. The pH of the solution was raised to 10 by drop-wise adding ammonium hydroxide after which 300 mg carbon black was added to the solution followed by 15 min of ultrasonication. The mixture was then heated in an oil bath to and kept at 70 °C for 20 h under constant mechanical stirring for platinum hydrolysis. The tungsten hydrolysis was performed by cooling the mixture to room temperature, adjusting the pH of the solution to 3 through drop-wise adding concentrated nitric acid while keeping the mixture under constant mechanical stirring for 2 h. Finally, the product was filtered, rinsed with de-ionized water, and dried in a furnace. The Pt/W powder was heat-treated at a temperature of 700 °C for 2 h under a flowing mixture of H_2/N_2 (1:10, v/v).

2.1.3. Reverse microemulsion method (RME)

The use of reverse microemulsion to prepare metallic and oxide tungsten as well as Pt alloys has been previously reported by this and other groups [29–33]. The synthesis of carbon-supported PtW alloy nanoparticle catalysts includes:

I. Preparation of a chloroplatinic acid microemulsion: A reverse microemulsion containing chloroplatinic acid was prepared by adding surfactant to a mixture of aqueous chloroplatinic acid and oil, ultrasonically blending for 15 min, and stirring at room temperature until a clear, stable reverse microemulsion was obtained. Both ionic surfactant (AOT) and non-ionic surfactant (Brij-30) were used in the synthesis.
II. Reduction of chloroplatinic acid within the reverse microemulsion: After forming the reverse microemulsion with chloroplatinic acid as the aqueous phase, hydrazine was drop-wise added to the microemulsion. The solution changed from yellow to black within a few minutes indicating the reduction of ionic Pt^{4+}. The solution was kept under constant mechanical stirring for an additional 15 min to ensure the complete reduction of Pt^{4+} to Pt^0.
III. Hydrolysis of the tungsten precursor within the reverse micelles: Following the reduction of Pt^{4+}, tungsten isopropoxide (50 mg ml^{-1} in isopropanol, Chemat Technology) was drop-wise added to the solution under constant mechanical stirring. The resulting solution was stirred for an additional 3 h to fully hydrolyze the tungsten isopropoxide.
IV. Dispersion on carbon-supports: An appropriate amount of carbon black was added to the solution and the mixture was stirred for 12 h to ensure a homogeneous dispersion of nanoparticles. Carbon-supported nanoparticles were precipitated by adding acetone, washed repeatedly with acetone and ethanol to remove the surfactants, and dried under blowing N_2 gas.
V. Heat treatment to complete surfactant removal and to alloy the nanoparticles: Heat treatments were conducted at elevated temperatures under a flowing mixture of H_2/N_2 gases (1:10, v/v). During the heat treatment process, remaining surfactants were removed from the nanoparticle surfaces, hydrous tungsten was reduced to metallic state, and alloyed PtW nanoparticle catalysts were formed.

The last two rows of Table 1 show the PtW/C catalysts prepared by the reverse microemulsion method. For example, a typical procedure for synthesizing 190 mg of carbon-supported 40 wt% PtW (51:49) nanoparticle catalysts by the reverse microemulsion method includes: ultrasonically mixing 5 g AOT, 1 ml de-ionized water, 0.2 mM chloroplatinic acid, and 50 ml cyclohexane or heptane for 15 min followed by constant mechanical stirring for an additional 2 h until a clear microemulsion solution was obtained; drop-wise adding 2.0 mM hydrazine hydrate to the above solution while keeping the solution under constant mechanical stirring for 15 min to ensure complete reduction of chloroplatinic acid; drop-wise adding 0.2 mM tungsten isopropoxide to the solution under constant stirring for 3 h to hydrolyze the tungsten isopropoxide; adding 114 mg carbon black to the solution under constant mechanical stirring for an additional 12 h; and finally, precipitating the reaction product by adding acetone followed by washing (acetone, ethanol, and water) repeatedly, filtration, drying, and heat treatment at a temperature of 700 °C for 2 h under a flowing mixture of H_2/N_2 (1:10, v/v).

2.2. Characterization

2.2.1. Transmission electron microscopy (TEM) and energy-dispersive spectroscopy (EDS)

The morphology and size of the carbon-supported PtW alloy nanoparticle catalysts were characterized by high-resolution TEM using a Hitachi HF-2000 field emission gun (FEG) TEM equipped with a Thermo Scientific ultra-thin window Si(Li) EDS. The average composition of the PtW alloy nanoparticles, as well as the compositions of individual nanoparticles, were determined by EDS. The nanoparticle samples for TEM-EDS analysis were prepared by dispersing the PtW/C powders in methanol and "looping" onto a lacey-carbon-coated copper grid followed by drying in air at room temperature.

2.2.2. X-ray diffraction (XRD)

The prepared carbon-supported PtW alloy nanoparticle catalysts were characterized by XRD using a Bruker powder diffractometer (a combination of model D8 Discover and D8 Advance) equipped with a scintillation detector using Cu Kα radiation. The diffraction patterns were recorded from $2\theta = 25–90°$ at a

scan rate of 0.02° per step and 5 seconds per point. The average particle sizes were estimated from diffraction peak broadening using the Debye–Scherrer formula:

$$d = \frac{0.9\lambda}{\Delta \cos(\theta)} \quad (1)$$

where λ is wavelength of the X-ray radiation, Δ is full width at half maximum of the diffraction peak, and θ is one half the angle corresponding to the peak position 2θ. It needs to be noted that XRD peak broadening delivers only the crystallite size, not particle size; but for spherical particles it gives a quick and close to real estimation.

2.2.3. Thermogravimetric analysis and differential scanning calorimetry (TGA-DSC)

Thermal analyses were performed by using a TA Instrument model SDT 2960 Simultaneous TGA–DSC. The samples were heated in air at a rate of 20 °C min^{-1} and alloy loading was calculated by the weight change after combustion of the carbon-support. The PtW alloy loadings on carbon-support were targeted to be close to a benchmark commercial Pt/C catalyst (~36.4 wt% Pt) for direct comparison with a baseline catalyst system.

2.2.4. Catalytic oxygen electroreduction activity

The catalytic oxygen electroreduction properties of the synthesized carbon-supported PtW alloy nanoparticle catalysts were measured in a 0.5 M H_2SO_4 electrolyte solution in a conventional three-compartment, three-electrode hydrodynamic system using a Pt mesh counter electrode, a saturated calomel reference electrode (SCE: 0.241 V versus reversible hydrogen electrode (RHE)), and a rotating disk working electrode. The working electrode (geometric surface area: 0.196 cm^2) was prepared by pipetting and uniformly distributing 15 μl of catalyst ink over the glassy carbon rotating disk electrode (RDE) tip surface. The catalyst ink was prepared by mixing 20 mg of carbon-supported PtW alloy catalyst, 20 ml of Milli-Q ultrapure water, and 1 ml of diluted Nafion solution (5 wt%, Aldrich) with a pulse ultrasonic probe. The electrolyte solution was de-aerated with high purity argon prior to electrochemical cleaning. Saturation with high purity oxygen was performed prior to the electrocatalytic activity screening. The potentials were controlled with respect to a SCE reference electrode by a Solartron potentiostat. All hydrodynamic polarization measurements were performed under a rotation speed of 2000 rpm with a scan rate of 5 mV s^{-1} in the anodic direction. Platinum mass activity was used for calculating relative activity as compared to a benchmark commercial Pt/C catalyst using the following relation [34–36]:

$$\frac{i_K}{m_{Pt}} = \frac{i_D - i}{i_D i m_{Pt}} \quad (2)$$

where i_K, i_D and i are the kinetic, diffusion limited, and total currents, respectively; and m_{Pt} is the mass of platinum used for the catalytic oxygen reduction reaction.

It should be noted that the catalytic activity of our benchmark Pt/C catalyst in 0.5 M H_2SO_4 (934.2 mA cm^{-2} mg$_{Pt}^{-1}$ at 800 mV with a half-wave potential of 800 mV) is about 2 times lower than literature data [35]. However, giving the elevated measuring temperature of 60 °C in Ref. [35], a factor of 2 is very reasonable. By comparing RDE measurements in different electrolytes or different concentrations of the same electrolyte, one can realize that electrolyte plays a critical role in catalytic oxygen electroreduction and it is important to compare the catalytic performance using the same electrolyte and the same concentration.

3. Results and discussion

Table 1 lists the characteristic parameters – synthesis method, atomic composition (Pt:W ratio), alloying temperature, average particle size (determined from XRD broadening), alloy loading (weight percent: wt%), mass activity (0.8 V) and half-wave potential relative to a benchmark Pt/C standard – of the PtW alloy nanoparticle catalysts fabricated for this study. Details pertaining to phase, morphology, particle size distribution, composition uniformity, and catalytic oxygen reduction activity for each of the wet chemical fabrication methods are given in the following sections.

3.1. PtW/C catalysts synthesized by the CBN method

Fig. 1(a) shows the XRD data of carbon-supported PtW alloy nanoparticle catalysts of different compositions synthesized by the CBN method and heat-treated at 700 °C in comparison with the XRD data of a benchmark Pt/C standard. All PtW/C catalysts exhibited a Pt face-centered cubic (fcc) structure (PDF card #04-0802) with a slight shift of the (1 1 1) reflection peaks to higher angle indicating a lattice contraction caused by the formation of the PtW alloys, i.e., incorporation of W into the Pt lattice. The peaks are assigned to the (1 1 1), (2 0 0), (2 2 0), (3 1 1), and (2 2 2) reflections. No phase segregation (pure Pt or pure W) was observed within the detection limitation of the XRD system. Average particle sizes for each catalyst were calculated from the peak broadening using Eq. (1) and are listed in Table 1.

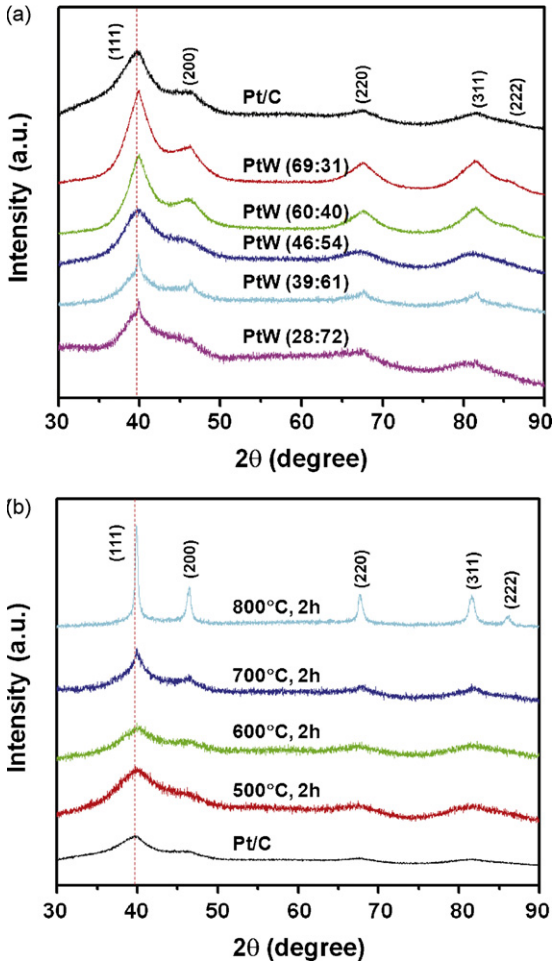

Fig. 1. XRD data for carbon-supported PtW alloy nanoparticles prepared by the CBN method in comparison with a benchmark Pt/C catalyst: (a) PtW alloyed at 700 °C with various Pt:W ratios; (b) PtW (52:48) alloyed at various temperatures.

Fig. 1(b) shows the XRD patterns of a carbon-supported PtW (52:48) alloy nanoparticle catalyst heat-treated at 500 °C, 600 °C, 700 °C, and 800 °C. The heat treatment temperature had a drastic influence on particle size and catalytic performance, as shown in Table 1. Heat treatments at 500 °C and 600 °C resulted in relatively poor catalytic performance, although the particle sizes remained small. Heat treatments at higher temperatures (above 800 °C) led to a significant increase in PtW particle size and crystallinity, as indicated by the sharp XRD reflection peaks, which also resulted in a reduction in catalytic performance. The optimum heat treatment temperature was found to be 700 °C, where small particle sizes were maintained and a peak in catalytic oxygen reduction activity was observed.

Fig. 2(a) displays a representative TEM micrograph of a carbon-supported PtW alloy nanoparticle catalyst prepared by the carbonyl method and heat-treated at 700 °C for 2 h. In the TEM image, the PtW nanoparticles appear as darkly imaging particles on the carbon-supports. All PtW alloy nanoparticles are predominantly spherical and uniformly dispersed on the carbon-supports. The nanoparticle sizes ranged from 1 nm to 3 nm with a very narrow size distribution, as determined from the TEM image (Fig. 2(b)). An average particle size of 1.6 nm was calculated, which is slightly smaller than the one determined from XRD peak broadening. At a high magnification, lattice fringes were observed for individual PtW nanoparticles, indicating that the alloy was well crystallized (see image inset of Fig. 2(a)). The XRD and TEM results clearly demonstrate that the CBN synthesis method is extremely effective for synthesizing small, uniformly dispersed, and well crystallized PtW alloy nanoparticles.

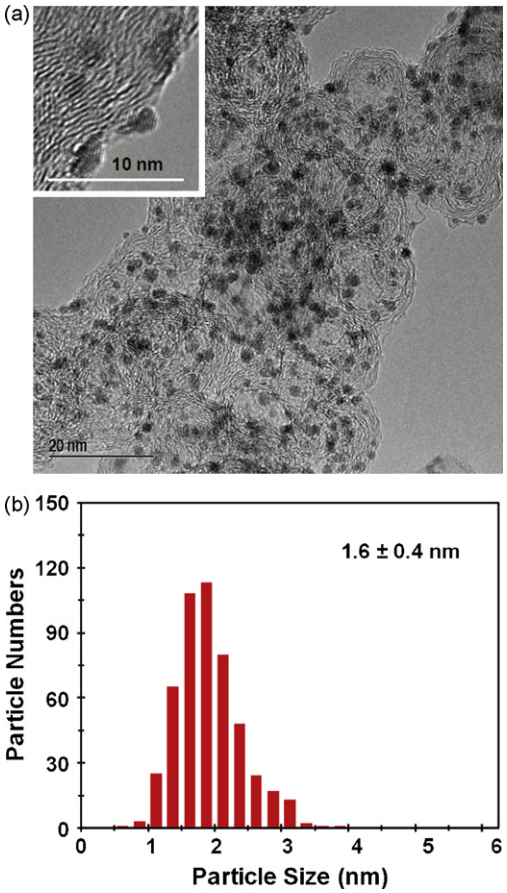

Fig. 2. (a) TEM image of a representative PtW alloy nanoparticle catalyst prepared by the CBN approach; high-resolution TEM image displays lattice fringes for individual nanoparticles consistent with Pt (inset); (b) the corresponding particle size distribution shows an average particle size of 1.6 nm.

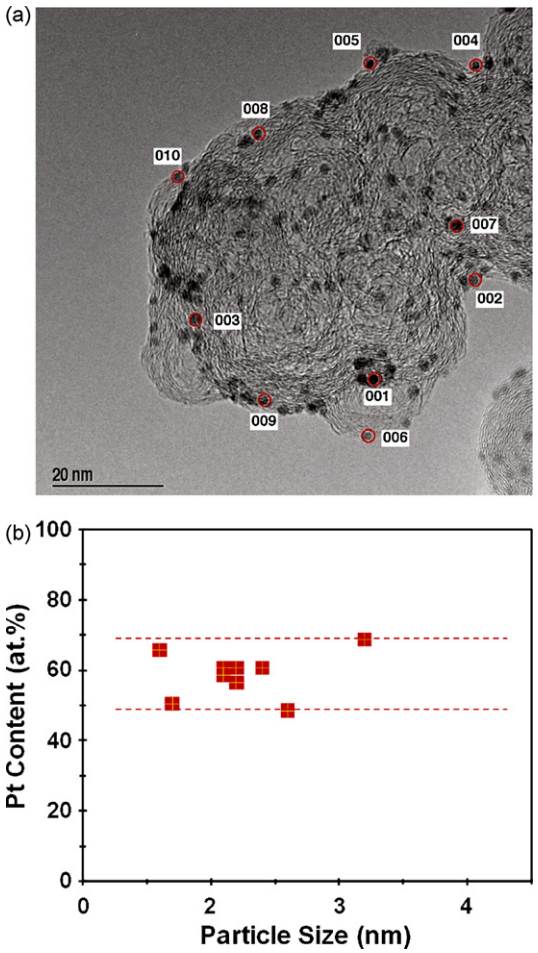

Fig. 3. (a) High spatial resolution TEM-EDS analysis of the compositions of individual PtW nanoparticles prepared by the CBN method; (b) the Pt atomic concentration of individual PtW nanoparticles as a function of particle size.

As demonstrated in our previous reports [20,37,38], micro-compositional uniformity is a critical issue in fabricating highly active Pt alloy electrocatalysts. The compositions of individual PtW nanoparticles were determined by high spatial resolution EDS performed using a field emission gun (FEG) TEM having a probe diameter of ~1.5 nm (Fig. 3(a)). The results of EDS analyses showed differences in the Pt:W ratio as a function of alloy particle size as shown in Fig. 3(b). The micro-compositions of individual PtW nanoparticles were relatively uniform with the Pt content varying between 50 at.% and 70 at.%. The macroscopic Pt:W ratio for this sample was 46:54, indicating that the tungsten was not completely alloyed (although excess/non-alloyed W was not observed via XRD or TEM). The composition difference due to unalloyed W may explain the relatively lower performance of the PtW nanoparticle catalyst as compared to thin film alloys [19], indicating a need for even better micro-compositional uniformity. Overall, the micro-compositional uniformity for the PtW alloy nanoparticles synthesized by the CBN method was fairly good in comparison to other binary alloy nanoparticles synthesized by conventional methods.

3.2. PtW/C catalysts synthesized by the HYD method

Fig. 4 displays the XRD data for carbon-supported PtW alloy nanoparticle catalysts of various Pt:W ratios synthesized by the hydrolysis method and heat-treated at 700 °C for 2 h. Broad diffraction peaks were observed that corresponded to fcc platinum. The average particle sizes for each PtW/C catalyst were estimated from

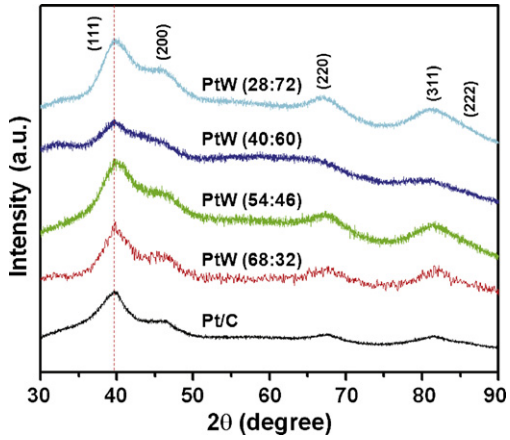

Fig. 4. XRD data for heat-treated carbon-supported PtW alloy nanoparticles of various Pt:W ratios prepared by the HYD method in comparison with a benchmark Pt/C catalyst.

peak broadening using Scherrer's equation and are listed in Table 1. From the XRD data shown in Fig. 4 and the corresponding average particle sizes, there was no distinctive difference between the hydrolysis and carbonyl synthesis methods.

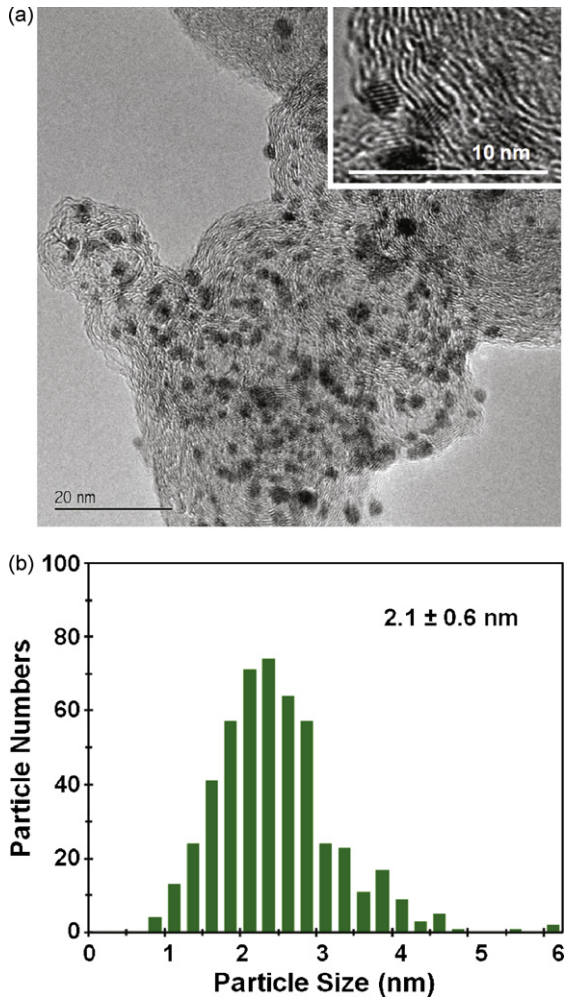

Fig. 5. (a) TEM image of a representative PtW alloy nanoparticle catalyst prepared by the HYD approach; high-resolution TEM image displays lattice fringes for individual nanoparticles consistent with Pt (inset); (b) the corresponding particle size distribution with an average particle size of 2.1 nm.

The TEM image of a representative PtW alloy nanoparticle catalyst prepared by the hydrolysis method and heat-treated at 700 °C for 2 h is shown in Fig. 5(a). PtW nanoparticles were well dispersed on the carbon-supports and no significant particle agglomeration was observed. The particle size distribution was slightly broader than that measured for the CBN-prepared PtW alloy nanoparticles, as shown in Fig. 5(b), resulting in a larger average particle size than the one synthesized by the carbonyl method, 2.1 nm versus 1.6 nm. At a higher magnification, lattice fringes were observed for individual PtW nanoparticles indicating that the alloy nanoparticles were well crystallized after heat treatment (see image inset of Fig. 5(a)).

Fig. 6(a) and (b) shows the EDS micro-compositional analyses of individual PtW nanoparticles fabricated by the hydrolysis method. The compositions of individual PtW nanoparticles were relatively uniform, however, the average composition of the nanoparticles, 50:50, is far from the nominal powder composition (28:72). One explanation for the discrepancy is that significant tungsten was not alloyed and remained amorphous. More experiments including inductively coupled plasma-optical emission spectroscopy (ICP-OES) are planned to clarify this issue.

Though it was reported that Pt nanoparticles could be fabricated from hydrolyzing Pt^{4+} in alkaline solutions in the presence of capping polymers [39], well-controlled Pt or PtW nanoparticles could also be synthesized by a similar hydrolysis approach without capping polymer or agency, as demonstrated here. Control synthesis without capping polymer/agency has the advantage of avoiding a subsequent capping polymer/agency cleanup procedure.

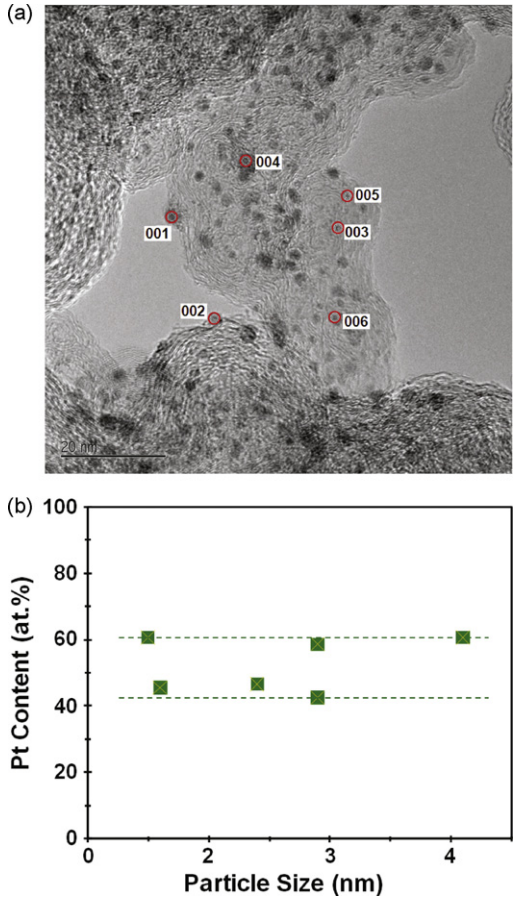

Fig. 6. (a) High spatial resolution TEM-EDS analysis of the compositions of individual PtW nanoparticles prepared by the HYD method; (b) the Pt atomic concentration of individual PtW nanoparticles as a function of particle size.

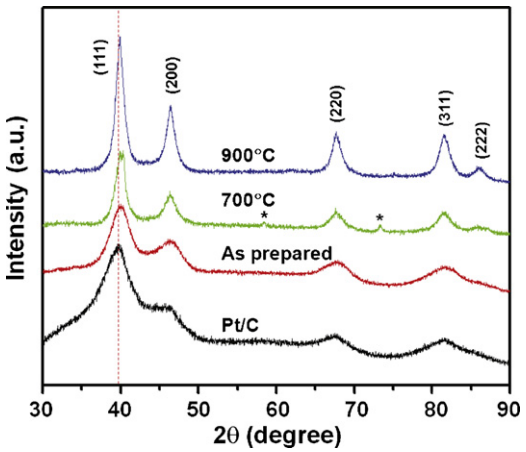

Fig. 7. XRD data for carbon-supported PtW alloy nanoparticles prepared by the RME method alloyed at different temperatures in comparison with a benchmark Pt/C catalyst. α-W peaks are marked by asterisks (*).

3.3. PtW/C catalysts synthesized by the RME method

Fig. 7 shows XRD data for carbon-supported PtW alloy nanoparticle catalysts synthesized by the RME method with AOT surfactants. The as-prepared PtW nanoparticle catalysts exhibited broad diffraction peaks similar to that of Pt/C standard. At 700 °C, additional diffraction peaks were observed corresponding to an α-W secondary phase, resulting from the reduction and crystallization of tungsten (hydrous) oxides, as reported previously [29]. After heat treatment at 900 °C, the α-W secondary phase vanished. In addition, the size of PtW nanoparticles increased significantly with temperature as evidenced by the increased sharpness of the XRD diffraction peaks in Fig. 7.

Fig. 8(a) displays a representative TEM micrograph of a carbon-supported PtW alloy nanoparticle catalyst prepared by the reverse microemulsion method and heat-treated at 700 °C for 2 h. The dispersion of PtW alloy nanoparticles on the carbon-supports was not as good as those obtained by the CBN or HYD methods. The average nanoparticle size (2.2 nm) and size distribution, however, were similar to the catalysts synthesized by the hydrolysis method (Fig. 8(b)). At a higher magnification, lattice fringes were also observed indicating that the alloy nanoparticles were well crystallized after heat treatment (see image inset of Fig. 8(a)).

Fig. 9(a) shows a TEM image of another PtW/C catalyst synthesized by the reverse microemulsion method. Similar to Fig. 8(a), the dispersion of the PtW nanoparticles on the carbon-support was not uniform. The compositions of ten nanoparticles ranging in size from 2 nm to 4 nm were analyzed, and are shown in Fig. 9(b). An excellent micro-compositional uniformity was achieved. However, the average individual nanoparticle composition (42:58) is slightly off the nominal powder composition (32:68), but in good agreement with the existence of α-W secondary phase determined by XRD.

3.4. Catalytic oxygen reduction activities of the carbon-supported PtW alloy nanoparticle catalysts in an acidic electrolyte

The catalytic activities towards molecular oxygen electroreduction of carbon-supported PtW alloy nanoparticle catalysts were measured by the hydrodynamic rotating disk electrode (RDE) technique in 0.5 M H_2SO_4. For quantitative comparisons, Tafel plots were created using the Levich–Koutecky relationship for Pt/C and PtW/C catalysts, the results of which are shown in Fig. 10(a). The mass activity is defined as the kinetic current normalized by the mass of platinum. All PtW/C catalysts showed enhanced mass ORR activities as compared to a benchmark Pt/C standard

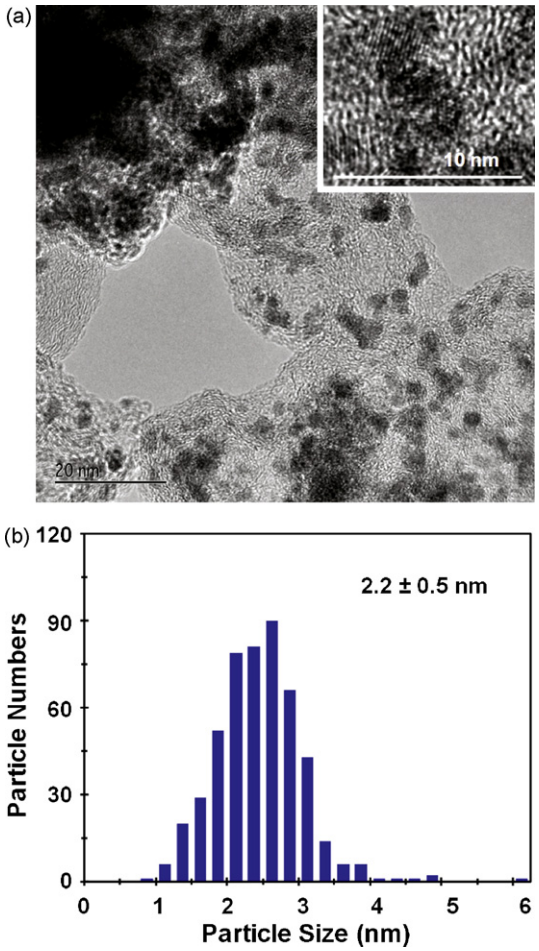

Fig. 8. (a) TEM image of a PtW alloy nanoparticle catalyst prepared by the RME approach; high-resolution TEM image displays lattice fringes for individual nanoparticles consistent with Pt (inset); (b) the corresponding particle size distribution with an average particle size of 2.2 nm.

(36.4 wt% loading). Fig. 10(b) compares relative mass activities of the carbon-supported PtW alloy nanoparticle catalysts synthesized by the three different approaches, CBN, HYD, and RME. The PtW/C catalysts prepared by the carbonyl method displayed the highest catalytic activity towards molecular oxygen electroreduction. A 3.4-fold enhancement in catalytic activity was achieved for this particular catalyst. PtW/C catalysts prepared by the hydrolysis and reverse microemulsion methods had very similar, but lower catalytic performance.

Fig. 11 displays the effect of alloy composition on the catalytic activity for PtW/C catalysts prepared by the wet chemical approaches and are compared with PtW thin film alloys (black dotted line) reported previously [19,20]. PtW catalysts prepared by the carbonyl method showed the best mass activity at ~40 at.% Pt, while those prepared by the hydrolysis method and reverse microemulsion method showed the best performance for alloy nanoparticles containing ~30 at.% Pt. However, all the PtW/C catalysts displayed a similar volcano plot behavior compared to the PtW thin film alloys, where the peak activity was observed for a Pt:W atomic ratio of 1:2. The data here clearly indicates that alloy composition plays an important role in catalytic oxygen electroreduction and that by carefully engineering alloy particles at the nanoscale, good agreement between thin film screening and nano-powder testing can be achieved. However, the activity differences could reflect that more efforts are needed to achieve even better micro-compositional uniformity in alloy nanoparticle catalysts.

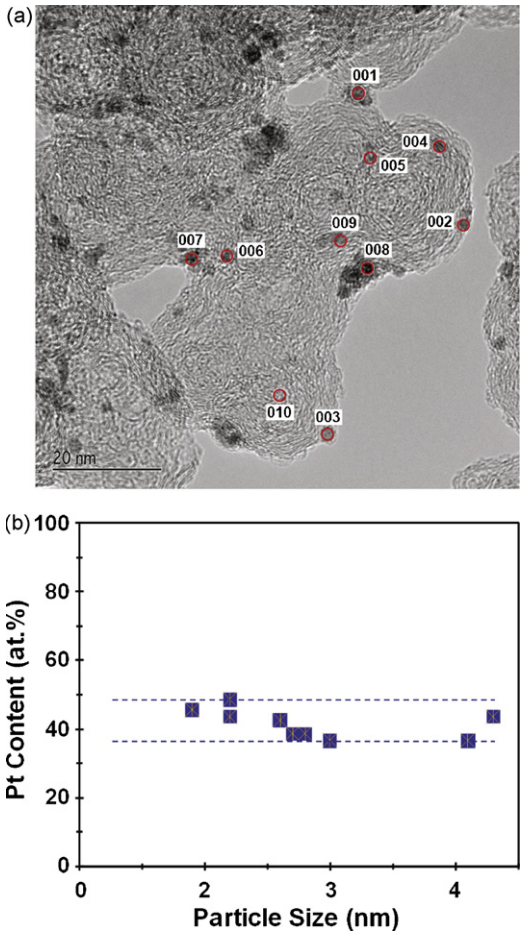

Fig. 9. (a) High spatial resolution TEM-EDS analysis for compositions of individual PtW nanoparticles prepared by the RME method; (b) the Pt atomic concentration of individual PtW nanoparticles as a function of particle size.

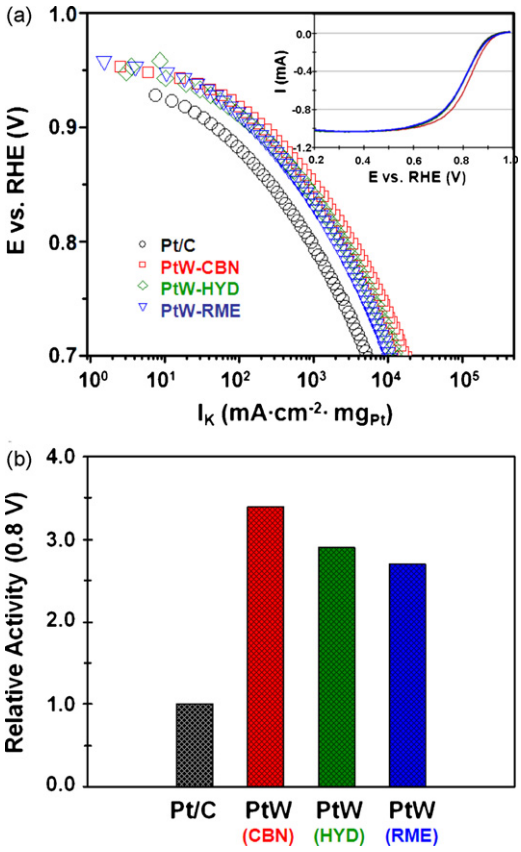

Fig. 10. (a) Tafel plots and *I–V* polarization curves (inset) of PtW alloy nanoparticle catalysts prepared by different wet chemical approaches; (b) the corresponding mass activities in comparison with a benchmark Pt/C standard. The nominal alloy compositions (Pt:W) are 39:61, 28:72, and 32:68 for PtW-CBN, PtW-HYD, and PtW-RME, respectively.

In addition to alloy composition, catalyst particle size also plays a crucial role in catalytic electroreduction of molecular oxygen. As has been demonstrated, the particle size, size distribution, particle dispersion (on carbon-supports), particle structure, and particle composition, are largely controlled by the synthetic fabrication method used and the alloying temperature Among the three synthetic methods described in this study, the carbonyl method generated the smallest nanoparticle sizes and the most uniform dispersion on the carbon-supports while the reverse microemulsion method produced the worst nanoparticle dispersion. The influence of heat treatment temperature on catalytic activity displayed a typical volcano relationship (see Table 1) resulting from the interplay of nanoparticle size and alloying effects. High annealing temperatures were necessary to promote the formation of PtW alloys leading to increased catalytic activity, however, rapid particle growth resulting from too high temperatures lead to a significant loss of electrochemically active surface area and hence a decrease in catalytic activity.

The last, yet most challenge, issue in control synthesis of alloy electrocatalysts is the micro-compositional uniformity of alloy nanoparticles. Among the three synthesis approaches developed here, the carbonyl approach displayed best micro-compositional uniformity with the average particle composition much closer to the nominal powder composition than those produced by hydrolysis and reverse microemulsion approaches. Generally speaking, higher alloying temperature is required if the micro-compositional uniformity cannot be achieved during a synthesis. For instance, the PtW nanoparticles produced by the reverse microemulsion method needed 900 °C to be alloyed while a relatively lower temperature (700 °C) was required to alloy PtW nanoparticles fabricated by the carbonyl method. Generally speaking, high alloying temperatures are due to the difficulty associated with the reduction of tungsten oxides and the long-range diffusion of Pt and W, while low alloying temperatures are a result of uniform micro-composition of alloy produced by the synthesis method. A combination of small particle size and uniform particle composition is the key to fabricate highly active electrocatalysts.

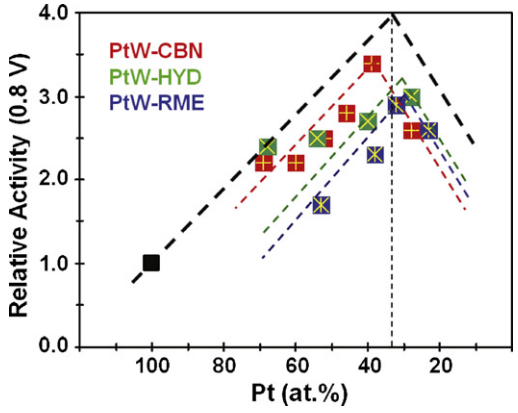

Fig. 11. The relative mass activities of PtW alloy nanoparticle catalysts prepared by different wet chemical methods as a function of Pt content as compared to the activities of PtW thin films (black dashed line).

The mechanisms for catalytic enhancement of platinum alloys have been studied extensively and various possible reasons have been proposed [40–45] including the role of alloy d-band centers, modification of platinum d-band vacancies, Pt–Pt interatomic distances, the effect of alloy facets, surface roughening due to leaching out of non-precious elements, and improved wettability. The volcano type plot of activity versus composition shown in Fig. 11 indicates there could be an optimal d-band vacancy in Pt leading to a maximum in activity [40]. The W atoms may function as adsorption sites for chemisorbed $OH_{ad}{}^{-}$ and O_2 in the dissociative adsorption of O_2 as observed in other transition metals [46]. This could influence the coverage of OH^{-} or O_2 on the surface of catalysts and hence the catalytic activity.

4. Conclusion

High-surface-area carbon-supported PtW alloy nanoparticle catalysts prepared by three different wet chemical approaches were investigated for catalytic oxygen reduction reaction in an acidic electrolyte. The synthesis method strongly influences particle sizes, size distributions, and micro-compositions of PtW alloy nanoparticles, resulting in differences in catalytic electroreduction of molecular oxygen. The carbon-supported PtW (39:61) alloy nanoparticle catalyst prepared by the carbonyl approach displayed the best catalytic activity under current scale of production with a 3.4-fold enhancement in mass activity as compared to a benchmark Pt/C catalyst.

Acknowledgments

Part of this research (KLM) was supported by the U.S. Department of Energy, Office of Hydrogen, Fuel Cells, and Infrastructure Technologies, as part of contract DE-AC05-00OR22725 with UT-Battelle, LLC. Microscopy Research (KLM) was supported by ORNL's SHaRE User Facility, sponsored by the Scientific User Facilities Division, Office of Basic Energy Science, the U.S. Department of Energy. The authors acknowledge Eric Kreidler for his kind assistance in preparing the manuscript.

References

[1] A.J. Appleby, Assessment of Research Needs for Advanced Fuel Cells, U.S. Department of Energy, 1985.
[2] S. Gottesfeld, T.A. Zawodzinski, in: R.C. Alkire, H. Gerischer, D.M. Kolb, C.W. Tobias (Eds.), Advances in Electrochemical Science and Engineering, Wiley–VCH, Weinheim, 1997, pp. 195–209.
[3] M.L. Perry, T.F. Fuller, J. Electrochem. Soc. 149 (2002) S59–S67.
[4] B.C.H. Steele, A. Heinzel, Nature 414 (2001) 345–352.
[5] W. Vielstich, A. Lamm, H.A. Gasteiger (Eds.), Handbook of Fuel Cells—Fundamentals, Technology and Applications, Wiley, West Sussex, 2003.
[6] F. Barbir, PEM Fuel Cells: Theory and Practice, Elsevier Academic Press, Boston, 2005.
[7] T. He (Ed.), Catalysts for Oxygen Electroreduction—Recent Developments and New Directions, Transworld Research Network, Kerala, 2009.
[8] V.R. Stamenkovic, B. Fowler, B.S. Mun, G. Wang, P.N. Ross, C.A. Lucas, N.M. Markovic, Science 315 (2007) 493–497.
[9] J. Zhang, K. Sasaki, E. Sutter, R.R. Adzic, Science 315 (2007) 220–222.
[10] J. Zhang, M.B. Vukmirovic, Y. Xu, M. Mavrikakis, R.R. Adzic, Angew. Chem. Int. Ed. 44 (2005) 2132–2135.
[11] Z. Chen, M. Waje, W. Li, Y. Yan, Angew. Chem. Int. Ed. 46 (2007) 4060–4063.
[12] N. Tian, Z.-Y. Zhou, S.-G. Sun, Y. Ding, Z.L. Wang, Science 316 (2007) 732–735.
[13] K. Gong, F. Du, Z. Xia, M. Durstock, L. Dai, Science 323 (2009) 760–764.
[14] B. Lim, M. Jiang, P.H.C. Camargo, E.C. Cho, J. Tao, X. Lu, Y. Zhu, Y. Xia, Science 324 (2009) 1302–1305.
[15] T. He, E. Kreidler, Phys. Chem. Chem. Phys. 10 (2008) 3731–3738.
[16] M. Götz, H. Wendt, Electrochim. Acta 43 (1998) 3637–3644.
[17] W. Zhou, Z. Zhou, S. Song, W. Li, G. Sun, P. Tsiakaras, Q. Xin, Appl. Catal. B 46 (2003) 273–285.
[18] M. Götz, H. Wendt, J. Appl. Electrochem. 31 (2001) 811–817.
[19] T. He, E. Kreidler, L. Xiong, E. Ding, J. Power Sources 165 (2007) 87–91.
[20] T. He, E. Kreidler, L. Xiong, J. Luo, C.J. Zhong, J. Electrochem. Soc. 153 (2006) A1637–A1643.
[21] J.B. Christian, S.P.E. Smith, M.S. Whittingham, H.D. Abruna, Electrochem. Commun. 9 (2007) 2128–2132.
[22] P. Trogadas, V. Ramani, J. Electrochem. Soc. 155 (2008) B696–B703.
[23] L. Xiong, T. He, Electrochem. Commun. 8 (2006) 1671–1676.
[24] N. Alonso-Vante, Fuel Cells 6 (2006) 182–189.
[25] A.J. Dickinson, L.P.L. Carrette, J.A. Collins, K.A. Friedrich, U. Stimming, Electrochim. Acta 47 (2002) 3733–3739.
[26] H. Yang, N. Alonso-Vante, C. Lamy, D.L. Akins, J. Electrochem. Soc. 152 (2005) A704–A709.
[27] H. Yang, W. Vogel, C. Lamy, N. Alonso-Vante, J. Phys. Chem. B 108 (2004) 11024–11034.
[28] L. Xiong, A. Manthiram, J. Mat. Chem. 14 (2004) 1454–1460.
[29] L. Xiong, T. He, Chem. Mater. 18 (2006) 2211–2218.
[30] D.H.M. Buchold, C. Feldmann, Chem. Mater. 19 (2007) 3376–3380.
[31] D.R.M. Godoi, J. Perez, H.M. Villullas, J. Electrochem. Soc. 154 (2007) B474–B479.
[32] V. Raghuveer, P.J. Ferreira, A. Manthiram, Electrochem. Commun. 8 (2006) 807–814.
[33] Y. Qian, W. Wen, P.A. Adcock, Z. Jiang, N. Hakim, M.S. Saha, S. Mukerjee, J. Phys. Chem. C 112 (2008) 1146–1157.
[34] U.A. Paulus, A. Wokaun, G.G. Scherer, T.J. Schmidt, V. Stamenkovic, N.M. Markovic, P.N. Ross, Electrochim. Acta 47 (2002) 3787–3798.
[35] U.A. Paulus, T.J. Schmidt, H.A. Gasteiger, R.J. Behm, J. Electroanal. Chem. 495 (2001) 134–145.
[36] V.G. Levich, Physicochemical Hydrodynamics, Prebtice Hall, Englewood Cliffs, NJ, 1962.
[37] T. He, in: P.D. Cozzoli (Ed.), Advanced Wet-chemical Synthetic Approaches to Inorganic Nanostructures, Transworld Research Network, Kerala, 2008.
[38] E. Ding, K.L. More, T. He, J. Power Sources 175 (2008) 794–799.
[39] M.T. Reetz, M.G. Koch, J. Am. Chem. Soc. 121 (1999) 7933–7934.
[40] A. Ruban, B. Hammer, P. Stoltze, H.L. Skriver, J.K. Norskov, J. Mol. Catal. A 115 (1997) 421–429.
[41] S. Mukerjee, S. Srinivasan, M.P. Soriaga, J. McBreen, J. Electrochem. Soc. 142 (1995) 1409–1415.
[42] V.M. Jalan, US Patent 4,202,934 (1980).
[43] M.T. Paffett, J.G. Beery, S. Gottesfeld, J. Electrochem. Soc. 135 (1988) 1431–1437.
[44] V. Stamenkovic, T.J. Schmidt, P.N. Ross, N.M. Markovic, J. Phys. Chem. B 106 (2002) 11970–11979.
[45] H.A. Gasteiger, S.S. Kocha, B. Sompalli, F.T. Wagner, Appl. Catal. B 56 (2005) 9–35.
[46] H. Yamazaki, S. Kamimizu, K. Hara, K. Sakamoto, Surf. Sci. 538 (2003) L505–L510.